Jurnal Teknologi

Full Paper

SAMARIUM ACTIVATED ABSORPTION AND EMISSION OF ZINC TELLURITE GLASS

Y.A. Tanko, M.R. Sahar, S.K. Ghoshal*

Advanced Optical Materials Research Group, Department of Physics, Faculty of Science, Universiti Teknologi Malaysia, 81310 UTM Johor Bahru, Johor, Malaysia

Article history
Received
10 February 2015
Received in revised form
30 May 2015
Accepted
30 June 2015

*Corresponding author
sibkrishna@utm.my

Graphical abstract

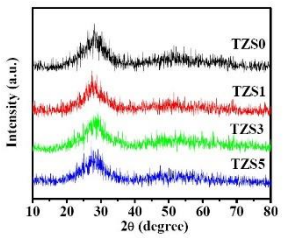

Abstract

Enhanced absorption and emission cross-sections of rare earth doped binary glasses are highly demanding for various photonic applications. Determining the right glass compositions with appropriate rare earth dopants remain challenging. Different microscopic mechanisms responsible for optical enhancement and quenching are not fully understood. In this view, we prepare a series of glasses with composition (80-x)TeO_2-20ZnO-(x)Sm_2O_3, where $0 \leq x \leq 1.5$ mol% using melt quenching technique. X-ray diffraction (XRD), Photoluminescence (PL) and Ultraviolet Visible Near-Infrared (UV-Vis-NIR) spectroscopic measurements are carried out to inspect the samarium concentration dependent absorption and emission features of the prepared glasses. Physical properties such as glass density and molar volume are found to be in the range 5.57-5.61 g cm^{-3} and 25.84-26.15 cm^3 mol^{-1}, respectively. XRD pattern verifies the amorphous nature of the prepared samples. The UV-Vis-NIR absorption spectra reveal nine peaks centered at 470, 548, 947, 1085, 1238, 1385, 1492, 1550 and 1589 nm. These bands arise due to $^6H_{5/2} \rightarrow {}^4I_{11/2}$, $^4G_{5/2}$, $^6F_{11/2}$, $^6F_{9/2}$, $^6F_{7/2}$, $^6F_{5/2}$, $^6F_{3/2}$, $^6H_{15/2}$, and $^6F_{1/2}$ transitions, respectively. PL spectra under the excitation of 452 nm display four emission bands centered at 563, 600, 644 and 705 nm corresponding to $^4G_{5/2} \rightarrow {}^6H_{5/2}$, $^6H_{7/2}$, $^6H_{9/2}$ and $^6H_{11/2}$ transitions of samarium ions. The mechanism of photoluminescence enhancement is identified, analyzed, and understood. A correlation between samarium concentration and optical response is established. This composition may be useful for fabricating various optical devices.

Keywords: Tellurite glass, samarium oxide, optical absorption, photoluminescence

Abstrak

Peningkatan penyerapan dan keratan rentas pancaran nadir bumi gelas binari amat diperlukan untuk pelbagai aplikasi fotonik. Untuk menentukan komposisi kaca yang betul dengan bahan dop nadir bumi yang sesuai kekal mencabar. Mekanisme mikroskopik yang berbeza bertanggungjawab untuk peningkatan optik dan pelindapkejutan tidak difahami sepenuhnya. Dalam konteks ini, kami menyediakan beberapa siri kaca dengan komposisi (80-x)TeO_2-20ZnO-(x)Sm_2O_3, dengan $0 \leq x \leq 1.5\%$ mol menggunakan teknik sepuh lindap. Pengukuran pembelauan sinar-X (XRD), Fotoluminensen (PL) dan UV-Vis-NIR spektroskopi dijalankan untuk memeriksa kesan kepekatan samarium bergantung pada ciri penyerapan dan pelepasan bagi kaca yang disediakan. Ciri fizikal seperti ketumpatan kaca dan jumlah molar, masing-masing yang disediakan ialah 5.57-5.61 g cm^{-3} dan 25.84-26.15 cm^3 mol^{-1}. Corak XRD mengesahkan sifat amorfus sampel bersedia. Penyerapan spectrum UV-Vis-NIR sembilan puncak berpusat di 470, 548, 947, 1085, 1238, 1385, 1492, 1550 dan 1589 nm. Jalur menunjukkan $^6H_{5/2} \rightarrow {}^4I_{11/2}$, $^4G_{5/2}$, $^6F_{11/2}$, $^6F_{9/2}$, $^6F_{7/2}$, $^6F_{5/2}$, $^6F_{3/2}$, $^6H_{15/2}$ dan $^6F_{1/2}$ serapan masing-masing terhasil dari peralihan peralihan. Spektra pancaran pada pengujaan 452 nm menunjukkan empat jalur pelepasan berpusat di 563, 600, 644 dan 705 nm sepadan dengan $^4G_{5/2} \rightarrow {}^6H_{5/2}$, $^6H_{7/2}$, $^6H_{9/2}$ dan $^6H_{11/2}$ prealihan ion samarium. Mekanisme peningkatan fotoluminesen dikenalpasti, dianalisa dan difahami. Korelasi antara kepekatan samarium dan tindak balas optik ditentukan. Komposisi ini akan berguna untuk mereka pelbagai peranti optik.

kata kunci: Tellurite glass, samarium oxide, optical absorption, photoluminescence

1.0 INTRODUCTION

In the past, optical properties of rare-earth doped glasses has been extensively studied for their numerous application in optical switching, solid state lasers, optical data storage, display monitor, sensors, etc. [1]. Lately, tellurite glasses became attractive due to their exceptional properties such as low phonon energy, high refractive index, low melting point, as well as good chemical and thermal stability [2-5]. When heavy metal oxides such as Pb, Mg, and Zn are being added to tellurite glass it shows reasonable changes in the physical and optical properties of the host. These glasses are promising optical material for luminescence in lasers and nonlinear optical materials.

The optical properties of Sm^{3+}-doped glasses are of special interest to many researchers including us. Trivalent Samarium ions known to exhibit broad emission bands due to $^4G_{5/2} \rightarrow {}^6H_J$ (J = 5/2, 7/2, 9/2, 11/2) transitions in preferred host matrix. Additionally, the phonon energies of hosts are not so critical to the reddish–orange emission at ~600 nm, because of the large energy difference of $^4G_{5/2}$ metastable level to its next lower lying level [6]. It is also well known that the intensities of emission bands of Sm^{3+} ion in glasses depend on its concentration and host glass composition [7]. To achieve optimum spectroscopic features, the overall composition dependent inspection is prerequisite for device applications.

In this communication, we report the careful synthesis of glasses via melt quenching method and their systematic characterizations for various physical as well as spectroscopic properties. Sm^{3+} ion concentration dependent variation in density, molar volume, refractive index, optical band gaps, and Urbach energy are presented. The absorption and emission spectral features of the prepared glasses are inspected as a function of Sm^{3+} contents. Results are analyzed, compared, and discussed using various mechanisms.

Table 1 Glass composition with codes, density, and molar volume

Glass codes	Mole percentage			Density(gcm^{-3})	Molar volume (cm^{3}mol^{-1})
	TeO_2	ZnO	Sm_2O_3		
TZS0	80.0	20	0.0	5.571	25.84
TZS1	79.7	20	0.3	5.578	25.91
TZS2	79.4	20	0.6	5.585	25.98
TZS3	79.1	20	0.9	5.599	26.01
TZS4	78.8	20	1.2	5.608	26.07
TZS5	78.5	20	1.5	5.613	26.15

2.0 EXPERIMENTAL

Following melt-quenching method glass samples having composition (80-x)TeO_2-20ZnO-xSm_2O_3, where x = 0, 0.3, 0.6, 0.9, 1.2 and 1.5 mol% are synthesized. About 15 grams of the analytical grade raw materials of tellurium dioxide (Sigma-Aldrich 99%), zinc oxide (ACROS 99%) and samarium oxide (Sigma-Aldrich 99.99%) were weighted and thoroughly grounded. Then, the powders are melted into a porcelain crucible by a raising heat electronic furnace at 800°C for 30 minutes before the melt was poured between two preheated steel molds in an alternative furnace and kept for 3 hours at 250°C. Finally, the samples were cooled down slowly to the room temperature. Samples were cut into desired sizes and polished for superior transparency. The glass compositions and corresponding labels together with their physical properties are summarized in Table 1.

The amorphous nature of the glasses was identified via x-ray diffraction (XRD) using a Burker D8 Advanced diffractometer with CuKa radiation source at 40 kV and 100 mA. Glass densities were measured using Archimedes principle with toluene as immersion liquid. The UV-Vis-IR absorption spectra of the samples were recorded using a Shimadzu UV-PC103 spectrophotometer with a resolution of 1 nm. PL measurements were performed by a Perkin-Elmer LS55 photoluminescence spectrometer with a resolution of 1 nm.

3.0 RESULTS AND DISCUSSION

Figure 1(a) displays the Sm_2O_3 concentration dependent variation of density. For all the glasses, the densities (ρ) are found to vary between 5.571-5.613 g/cm^3 with an estimated error of ±0.001 g/cm^3. The measured values of density and molar volume are in agreement with other reports [8, 9]. The increase in glass density with the increase of Sm^{3+} ion concentration is attributed to the occupation of Sm_2O_3 (higher molecular weight) in the tellurium matrix. Figure 1(b) shows the increase in molar volume with

the increase of Sm_2O_3 contents is interpreted in terms of the elongation in the bond length or the inter-atomic spacing between the atoms [10].

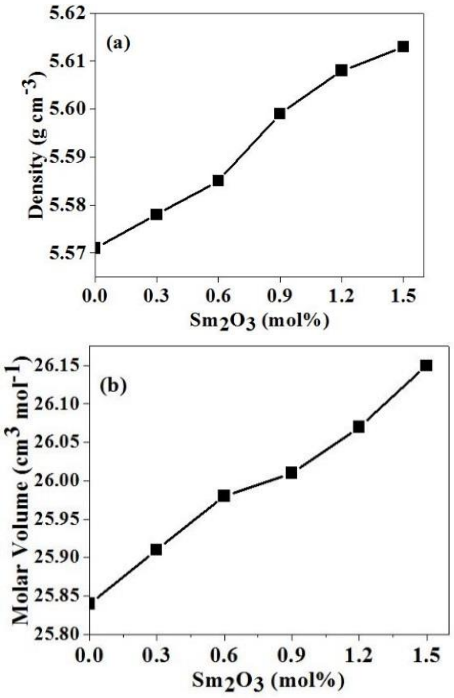

Figure 1 (a) Sm^{3+} ion concentration dependent glass density and (b) Molar volume versus concentration of Sm^{3+} ions.

Figure 2 shows the XRD pattern of the samples with and without samarium oxide. The glasses do not reveal any discrete or continuous sharp peak but show a broad hunch in the diffraction pattern. The absence of any sharp peaks between 2θ = 10-80° and the presence of a broad hump between 20° and 35° confirms the amorphous nature of the glass as observed by others [11, 12].

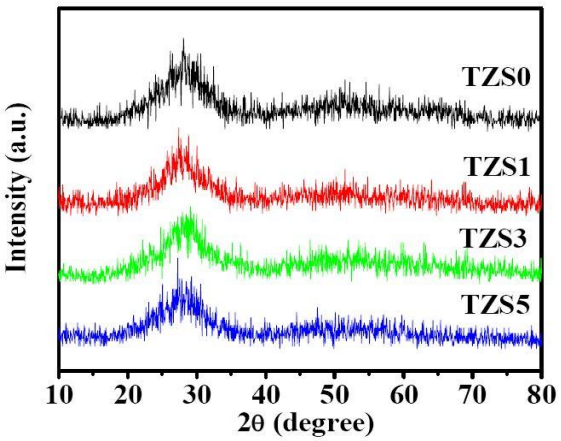

Figure 2 XRD patterns of all samples.

Figure 3 presents the UV-Vis-NIR absorption spectra of all samples. The appearance of nine absorption bands centered at 470, 548, 947, 1085, 1238, 1385, 1492, 1550 and 1589 nm are assigned to the excitations from $^6H_{5/2}$ ground state to $^4I_{11/2}$, $^4G_{5/2}$, $^6F_{11/2}$, $^6F_{9/2}$, $^6F_{7/2}$, $^6F_{5/2}$, $^6F_{3/2}$, $^6H_{15/2}$ and $^6F_{1/2}$ exited states of Sm^{3+} ions, respectively. Our results are in conformity with others observation [13-15].

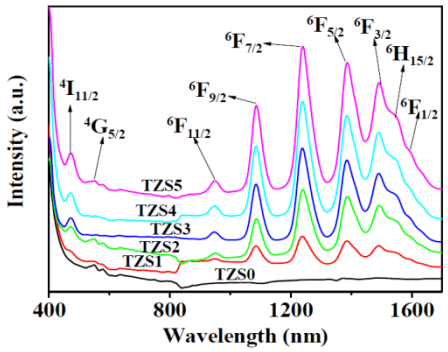

Figure 3 Absorption spectra for Sm^{3+}-doped zinc tellurite glasses.

Figure 4 displays the room temperature luminescence spectra of all samples in the region of 550 – 700 nm under 452 nm excitation wavelengths. The emission spectra exhibit four significant emission bands centered at 563, 600, 644 and 705 nm ascribed to $^4G_{5/2}$ → $^6H_{5/2}$, $^6H_{7/2}$, $^6H_{9/2}$ and $^6H_{11/2}$ transitions, respectively as reported earlier [12, 16, 17]. The band at 600 nm corresponding to $^4G_{5/2}$ → $^6H_{7/2}$ transition manifests strong orange luminescence followed by $^4G_{5/2}$ → $^6H_{9/2}$ transition at 644 nm with strong red emission. However, the peak at 563 nm corresponding to $^4G_{5/2}$ → $^6H_{5/2}$ displays weak green luminescence. Lastly, $^4G_{5/2}$ → $^6H_{11/2}$ (705 nm) is assigned to the weak red luminescence.

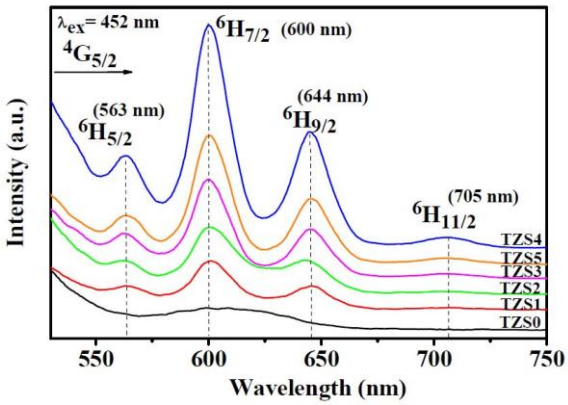

Figure 4 Emission spectra for Sm^{3+}-doped zinc tellurite glasses.

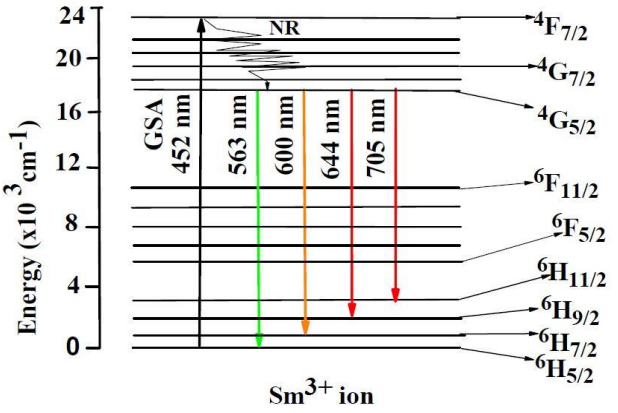

Figure 5 Partial energy level diagram of Sm^{3+} ion fluorescence emission.

Different mechanisms involved in the luminescence process in explained via the partial energy level diagram of samarium ion as shown in Figure 5. For the ground state $^6H_{5/2}$, absorption occurs which is referred to as ground state absorption (GSA) for which electrons is lifted to the excited energy level. Some energy (nonradioactive) is released as a result of electronic vibrational relaxation between the excited energy levels. From there, internal conversion (transition to the lowest excited energy level $^4G_{5/2}$) occurs and excited electrons returns back to $^6H_{5/2}$, $^6H_{7/2}$, $^6H_{9/2}$ and $^6H_{11/2}$ transitions thereby emitting green, intense orange and red fluorescence.

4.0 CONCLUSION

We demonstrated the effects of Sm^{3+} ion concentration on the absorption and the luminescence features of zinc tellurite glasses. A correlation between Sm^{3+} contents and physical properties is established. The absorption spectra exhibited nine absorption bands corresponding to the transition from ground level $^6H_{5/2}$ to the various excited state of Sm^{3+} ions in the range 400-1800 nm. The luminescence spectra displayed four emissions peaks centered at 563, 600, 644, and 705 nm which are assigned to $^4G_{5/2} \rightarrow {}^6H_{5/2}$, $^6H_{7/2}$, $^6H_{9/2}$ and $^6H_{11/2}$ transitions, respectively. The excellent features of the results suggest that Sm^{3+} doped zinc tellurite glasses of the present composition are suitable for the development of solid state lasers and other photonic devices.

Acknowledgement

The authors gratefully acknowledge the financial support from UTM and Malaysian Ministry of Education through Vot.05H36, 05H45 (GUP) and 4F319, 4F424 (FRGS).

References

[1] Agarwal, A., Pal, I., Sanghi, S. and Aggarwal, M. P. 2009. Judd–Ofelt Parameters And Radiative Properties Of Sm^{3+} Ions Doped Zinc Bismuth Borate Glasses. *Optical Materials*. 32,339-344.

[2] El-Mallawany, R. A. H. 2002. *Tellurite Glasses Handbook: Physical Properties And Data*. CRC Press.

[3] Wang, J.S., Vogel, E.M. and Snitzer, E. 1994. Tellurite Glass: A New Candidate For Fiber Devices. *Optical Materials*. 3: 187-203.

[4] Thomos, P. A. 1998. The Crystal Structure And Absolute Optical Chirality Of Paratellurite, A-TeO_2. *Journal Of Physics C: Solid State Physics*. 21: 4611-4627.

[5] Kumar, G., De la Rosa, E. and Desirena, H. 2006. Radiative And Non-Radiative Spectroscopic Properties Of Er^{3+} Ion In Tellurite Glass. *Optics Communications*. 260: 601-606.

[6] Farries, M. C., Morkel, P.R. and Townsend, J.E. 1998. Samarium Ion Doped Glass Laser Operating At 651nm. *Electronics Letters*. 24: 709-711.

[7] Jamalaiah, B., Kumar, J. S., Babu, A. M., Suhasini, T. and Moorthy, L. R. 2009. Photoluminescence Properties Of Sm^{3+} In LBTAF Glasses. *Journal Of Luminescence*. 129: 363-369.

[8] Yusoff, N. and Sahar, M. R. 2015. Effect Of Silver Nanoparticles Incorporated With Samarium-Doped Magnesium Tellurite Glasses. *Physica B: Condensed Matter*. 456: 191-196.

[9] Dousti, M .R., Sahar, M. R., Ghoshal, S.K., Amjad, R.J. and Samavati A. R. 2013. Effect of AgCl On Spectroscopic Properties Of Erbium Doped Zinc Tellurite Glass. *Journal of Molecular Structure*. 1035: 6-12.

[10] Hager, I. and El-Mallawany, R.A.H. 2010. Preparation and structural studies in the (70− x) TeO_2–$20WO_3$ –$10Li_2O$–xLn_2O_3 glasses. *Journal Of Materials Science*. 45: 897-905.

[11] Selvaraju, K. and Marimuthu, K. 2013. Structural And Spectroscopic Studies On Concentration Dependent Sm^{3+} Doped Boro-Tellurite Glasses. *Journal of Alloys and Compounds*. 553: 273-281.

[12] Dousti, M. R., Ghoshal, S. K., Amjad, R. J., Sahar, M. R., Nawaz, F. and Arifin, R. 2013. Structural And Optical Study Of Samarium Doped Lead Zinc Phosphate Glasses. *Optics Communications*. 300: 204-209.

[13] Nawaz, F., Sahar, M.R., Ghoshal, S.K., Awang, A. and Ahmed, I. 2014. Concentration Dependent Structural And Spectroscopic Properties of Sm^{3+}/Yb^{3+} Co-Doped Sodium Tellurite Glass. *Physica B: Condensed Matter*. 433: 89-95.

[14] Som, T. and Karmaker, B. 2008. Infrared-To-Red Upconversion Luminescence In Samarium-Doped Antimony Glasses. *Journal Of Luminescence*. 128: 1989-1996.

[15] Nawaz, F., Sahar, M. R. and Ghoshal, S. K. 2014. The Influence of Yb^{3+} Co-Doping on Optical Properties of Sm^{3+}-Doped Sodium Tellurite Glasses. *Advanced Materials Research*. 895: 359-362.

[16] Maheshvaran, K., Linganna, K. and Marimuthu, K. 2011. Composition Dependent Structural And Optical Properties Of Sm^{3+}Doped Boro-Tellurite Glasses. *Journal of Luminescence*. 131: 2746-2753.

[17] Bolundut, L., Culea, E., Borodi, G., Stefan, R., Munteanu, C. and Pascuta, P. 2015. Influence Of Sm^{3+}: Ag Codoping On Structural And Spectroscopic Properties Of Lead Tellurite Glass Ceramics. *Ceramics International*. 41: 2931-2939.